Characterization of Chromatic Banding Artifact for Secondary Colors in a Polychrome Electrophotographic Process

Mu-Chih Chen[1], George T.-C. Chiu[1] and Jan P. Allebach[2]
[1]School of Mechanical Engineering
[2]School of Electrical and Computer Engineering
Purdue University
West Lafayette, Indiana, USA

Abstract

Several passive and active[1-3] banding compensation strategies have been proposed in recent literatures for monochrome EP processes. In these studies, quasi- periodic contrast variations can be effectively reduced. For polychrome EP process, in which multiple color layers are superimposed on top of one another, Klassen and Goodman[4] have shown the dependence of contrast sensitivity on variation in chromatic channels such as a* and b*. Chromatic bandings are quasi-periodic gratings with variation in chromatic channels. Chromatic banding may still be perceivable when the achromatic banding on individual color layers has been reduced to under the threshold. The perceptibility of chromatic banding is dependent on the primary colors of the platform. Before a softcopy psychophysics experiment was conducted, a set of tone curves and a model of the mixing of two primary colors, excluding the black, were constructed according to a 4-color EP printer. The psychophysics study confirmed that even if the sinusoidal gratings (in L*) on each individual primary color layer is under the human visual system (HVS) threshold, superimposing one on top of another can increase the perceptibility of the composite gratings. These results will be much valuable to ongoing efforts to reduce chromatic banding.

Introduction

Electrophotography (EP) is the basic imaging process used in paper copiers and laser printers. For a typical EP process, the image quality strongly depends on the six basic steps, i.e. charging, exposure, developing, transferring, fusing, and cleaning. Thus, any factor affecting those above processes would definitely affect the image quality. Wulich and Kopeika[6] pointed out that mechanical vibration would limit the resolution of an EP process. Among various well-known image artifacts, halftone banding due to scan line spacing variation is one of the most visible defects, which appears as light and dark streaks across a printed page perpendicular to the process direction.

Some literature has been devoted to the modeling and analysis of banding in EP process. Burns et al.[7] discovered that laser beam positioning error would result in undesirable image noise, which degrades the image quality. Melnychuck et al.[8] identified strong correlation between the scan line spacing variation and the occurrence of banding. Loce et al.[9] modeled vibration-induced halftone banding in laser printers. Although scan line spacing and reflectance variation are shown to be direct contributor of banding, a model of the human visual system (HSV) is needed to reflect the actual banding perceived by human eyes. The contrast sensitivity function (CSF) is one of such models that help capturing the modulation transfer function (MTF) of human eyes on perceiving spatial information. Several researches have contributed to the analysis and synthesis of the CSF function, which has been used by other researchers to quantify perceived image quality.[10,11] The band-pass-like CSF function reveals the fact that mid-frequency disturbances have greater impact on perceived banding so that a banding cancellation scheme should supply its reduction effort mainly on bandings located in this frequency region.

In this paper the information similar to the CSF for chromatic banding is investigated. Goodman[5] has proposed curves similar to the CSF in single primary color layers, but no information about the superimposition of two or more color layers was provided. In this study, we have developed softcopy psychophysical experiments to characterize human visual perception of chromatic banding of secondary colors that are generated by superimposing two primary colors each with different levels of banding. The goal is to understand the relationship between the visual chromatic banding threshold for secondary colors and the corresponding thresholds for the composing colors. This information will help determine whether reducing banding for individual color planes to below threshold is a reasonable target or more involved consideration is needed.

The remaining of the paper is organized as follows. The characterization of superimposing two primary colors for a color EP printer and the softcopy emulation system is presented in the next section. The third section describes psychophysical experiments followed by the discussion of the experimental procedure. Experimental results are then presented. A summary of the findings concludes the last section.

Color Modeling of the Target EP Engine

System Description

The target platform is a typical inline four-color chromatic EP engine, of which the structure is shown in Figure 1. Black, Cyan, Magenta, and Yellow toner layers are transferred onto paper consecutively. Therefore, they superimpose on one another. The formation of each layer has its own corresponding EP process. Because these processes typically have similar mechanisms, the disturbance acting on the four OPC drums are also similar. It results in similar banding characteristics on all the color layers Figure 2 shows the speed spectrums of the four OPC drums measured from the target EP engine. The main peaks appear in all 4 spectrums at the same frequencies.

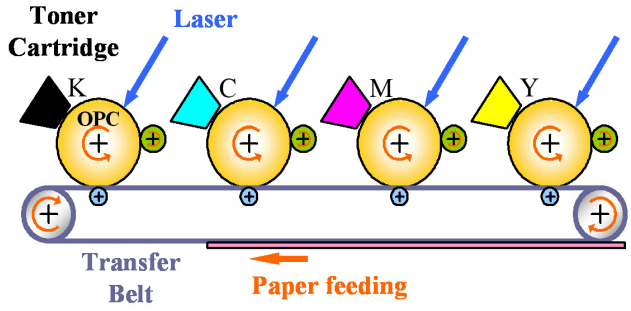

Figure 1. In-line 4-color chromatic laser printer structure

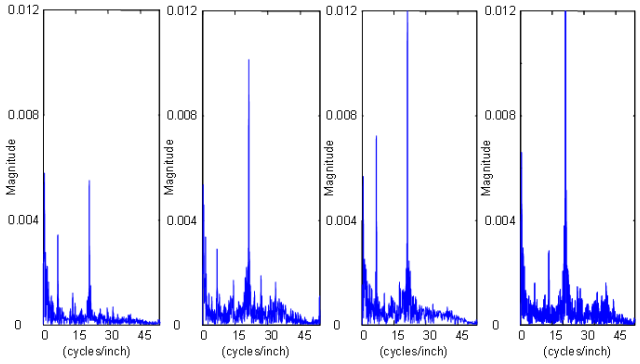

(a) Cyan *(b) Yellow* *(c) Magenta* *(d) Black*

Figure 2. Speed spectrums of the four OPC drums

Printer Tone Curves

Each color plane has its own tone curve. Different color toners in different amount result in different CIELAB values. Because we want to use a softcopy psychophysics experiment to investigate the chromatic banding, when multiple color layers superimpose on one another, the CIELAB values of the resultant color has to be predictable before the softcopy experiment can be conducted. To measure the tone curves as well as the mixing of two primary colors, a PostScript test page shown in Figure 3 was designed and printed with the target EP engine. On the test page there are three groups of patches. In each group, the top row and the left column consist of only primary colors, excluding the black. Each of the other patches is the mixing of its corresponding primary color in the top row and the primary color in the left column. Note that the amounts of the primary color toners in each mixed patch have been adjusted to match the primary color column and row. Note that the embedded color table in the printer has been taken into consideration on this test page.

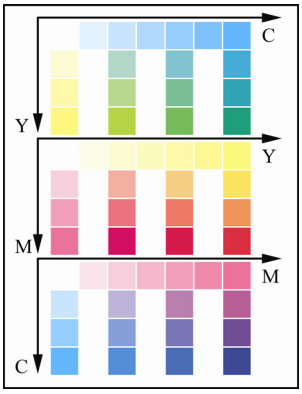

Figure 3. Test page used to measure the tone curves and to model the mixing of two primary colors excluding the black

After the test pages are printed, the CIELAB values of the color patches on the test page were measured by a GretagMacbeth SpectroEye Photometer. Note that the CIELAB values measured in this paper are all with respect to the D65 lighting source. The tone curves shown in Figure 4 were measured from the primary color rows on the test pages. They were fitted with curves in the 3-dimensional space. These curves can be generally formulated by

$$\begin{bmatrix} a^*_{prim\_color} \\ b^*_{prim\_color} \end{bmatrix} = \tilde{f}_{prim\_color}(L^*_{prim\_color}) \qquad (1)$$

where prim_color can be substituted with any of Cyan, Yellow, or Magenta. This is a nonlinear mapping from an EP engine's CMY space to the CIELAB space.

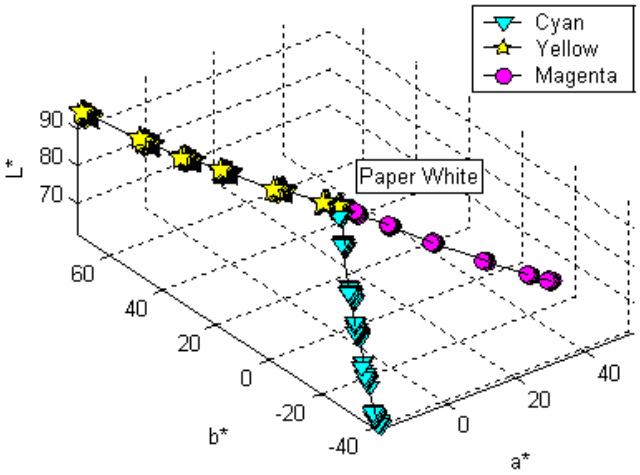

Figure 4. Tone curves of the target EP engine

Superimposition of Two Primary Colors

To model how two primary colors superimpose for the color EP printer, the CIELAB values of the mixed color patches on the test page were measured. The measurements were fitted with the subtractive color mixing process defined by

$$Absorptance_{A+B} = Absorptance_{A} + Absorptance_{B}$$

$$\Leftrightarrow \left(\begin{bmatrix} L^*_{paper} \\ a^*_{paper} \\ b^*_{paper} \end{bmatrix} - \begin{bmatrix} L^*_{A+B} \\ a^*_{A+B} \\ b^*_{A+B} \end{bmatrix} \right)$$

$$= \left(\begin{bmatrix} L^*_{paper} \\ a^*_{paper} \\ b^*_{paper} \end{bmatrix} - \begin{bmatrix} L^*_{A} \\ a^*_{A} \\ b^*_{A} \end{bmatrix} \right) + \left(\begin{bmatrix} L^*_{paper} \\ a^*_{paper} \\ b^*_{paper} \end{bmatrix} - \begin{bmatrix} L^*_{B} \\ a^*_{B} \\ b^*_{B} \end{bmatrix} \right)$$

$$\Leftrightarrow \begin{bmatrix} L^*_{A} \\ a^*_{A} \\ b^*_{A} \end{bmatrix} + \begin{bmatrix} L^*_{B} \\ a^*_{B} \\ b^*_{B} \end{bmatrix} - \begin{bmatrix} L^*_{paper} \\ a^*_{paper} \\ b^*_{paper} \end{bmatrix} = \begin{bmatrix} L^*_{A+B} \\ a^*_{A+B} \\ b^*_{A+B} \end{bmatrix} \quad (2)$$

where $L^*_{\bullet}$ represents the L^* value of $\bullet$, and A and B denote the two primary colors that are mixed together. The L_∞ norm prediction errors were found to be bounded by 4 ΔE when the PostScript densities were below 50%.

Psychophysics Experimental Setup

Hardware Setup

For the softcopy psychophysics experiment, we used a 21-inch BARCO Reference Calibrator V Wave II monitor, which can be calibrated in 25 zones using a BARCO OPTISENSE calibration device to guarantee color uniformity to be around 1 ΔE. The resolution was set to 1600x1200 and the refresh rate at 85 Hertz. The gammas for the RGB phosphors were set to 2.2 for all three channels. The color temperature was set to 6500K. The CIE xyz values of each of the RGB phosphors were recorded.

A head-chin rest was affixed to the table, 14 inches away in front of the monitor. This was to fix the viewing distance for all the subjects.

Software Environment

The experiment program was coded in MATLAB R13 Graphical User Interface Design Environment. In the program, a Settings option lets the researcher adjust a horizontal and a vertical target until they measure exactly 5 inches. This step calibrates the monitor's horizontal and vertical resolutions in PPI (pixels-per-inch), which can be distorted after the monitor's geometry adjustment. These two values are taken into account when the test patterns are being generated to ensure correct banding spatial frequencies in cycles per inch.

The program that generates the test patterns computes the RGB values that need to be sent to the calibrated monitor from the desired CIE L* values. It first computes a* and b* from the desired L* according to the mapping, Eq. (1), obtained from the previous section. Then by applying the following transformations in sequence

$$\begin{bmatrix} X \\ Y \\ Z \end{bmatrix} = \begin{bmatrix} x_w \cdot \left(\frac{a^*}{500} + \frac{L^*+16}{116}\right)^3 \\ y_w \cdot \left(\frac{L^*+16}{116}\right)^3 \\ z_w \cdot \left(\frac{L^*+16}{116} - \frac{b^*}{500}\right)^3 \end{bmatrix} \quad (3)$$

$$M = \begin{bmatrix} x_R & x_G & x_B \\ y_R & y_G & y_B \\ z_R & z_G & z_B \end{bmatrix} \cdot diag\left(\begin{bmatrix} x_R & x_G & x_B \\ y_R & y_G & y_B \\ z_R & z_G & z_B \end{bmatrix}^{-1} \cdot \begin{bmatrix} x_w \\ y_w \\ z_w \end{bmatrix} \right) \quad (4)$$

$$\begin{bmatrix} \tilde{R} \\ \tilde{G} \\ \tilde{B} \end{bmatrix} = M^{-1} \cdot \begin{bmatrix} X \\ Y \\ Z \end{bmatrix}, \quad (5)$$

$$\begin{bmatrix} R \\ G \\ B \end{bmatrix} = 2^{16} \cdot \begin{bmatrix} \tilde{R}^{1/\gamma_R} \\ \tilde{G}^{1/\gamma_G} \\ \tilde{B}^{1/\gamma_B} \end{bmatrix}, \quad (6)$$

where the notations are defined in Table 1, the program converts the CIE LAB values into the monitor's 16-bit RGB values.

Nature of Subject Population

The subjects who participated in the experiment were students recruited from the School of Mechanical Engineering at Purdue University. They all have normal vision, especially color vision.

Table 1. List of terms in Equations (3) through (6)

L^*, a^*, b^*	Desired CIE LAB values
X, Y, Z	CIE XYZ values
x_w, y_w, z_w	CIE xyz values of the white point
M	Transformation matrix from linear RGB space to CIE XYZ space
x_R, y_R, z_R	CIE xyz values of the monitor's red phosphor
x_G, y_G, z_G	CIE xyz values of the monitor's green phosphor
x_B, y_B, z_B	CIE xyz values of the monitor's blue phosphor
$\tilde{R}, \tilde{G}, \tilde{B}$	Linear RGB values before gamma correction
$\gamma_R, \gamma_G, \gamma_B$	Gamma values of the monitor's three phosphors (all set to 2.2)

Experiment Procedures

In this experiment only one banding frequency, which is 13.48 cycles per inch, was tested. This particular banding frequency is one of the most obvious banding components in the target EP engine. Figure 2 shows the speed spectrums of the target EP engine's four OPC drums. Because the mechanisms for all the four OPC drums are similar, they also have similar banding characteristics. There are other banding frequencies, but in this study only one was picked for the experiment. The same procedure can simply be duplicated for the other banding frequencies.

PART I: Banding on a Primary Color Layer

The psychophysics experiment consists of six sub-experiments. The first three test a subject's sensitivities to bandings in the cyan, yellow, and magenta planes, respectively. For each of these sub-experiments 2-inch squared test patterns are generated before the tests begin. The test patterns include a catch pattern, which intends to catch those false positives from the subjects, and 7 levels of banding patterns. The catch pattern does not have any banding in it. It is only a uniform field of primary color which corresponds to a 50% PostScript density defined in the test page shown in Figure 3. The color of the catch pattern is also the mean color of all the 7 banding patterns. The levels of the banding patterns are defined by the fluctuation amplitude ΔL*, although the fluctuation is really along the 3-D tone curve shown in Figure 4. It is the toner mass variation. In other words, the L^* at every position is computed by

$$L^*(y) = L_0^* + \Delta L^* \cdot \sin(2\pi f y + \phi) \tag{7}$$

where L_0^* is the nominal L^* value, f is the banding frequency, y is the position in the printer process direction, and ϕ is the phase. The a* and b* value at every position are computed from the L* at the same position based on Eq. (1).

Finally a 2-D Gaussian filter with 0.5-inch stand deviation is applied to each banding pattern for L*, a*, and b* to form a Gabor patch, which limits the bandwidth. Figure 5 shows a sample test pattern in magenta. Note that the banding level and frequency in Figure 5 has been adjusted for better illustration on paper.

Figure 5. A sample test pattern in magenta

With the test patterns prepared, 10 catch trials plus 10 trials per banding pattern (totally 80 trials) are presented to the subject in random orders at random positions on the screen. The subject is asked to respond whether s/he sees banding on the presented test pattern. There is no time limit before the subject makes a choice. The responses are recorded and fitted with a cumulative Gaussian curve. The same procedure repeats for all three primary colors. Subject HH's results, for example, are shown in Figure 6. The absolute threshold (AL) for each of the primary colors is the banding level at which the subject's response reaches the 50th percentile. These three AL's were used for the second part of the experiment.

PART II: Banding on Superimposed Color Layers

The other three sub-experiments test the perceptibility of banding on the images formed by superimposing two primary color layers, which both have banding in them. Generating the test patterns in this part follows the model of the superimposition of two primary color layers of the EP printer defined in Eq. (2). Similar to PART I, a catch pattern and several banding patterns are generated based on

$$\begin{aligned} L_A^*(y) &= L_{Ao}^* + r \cdot AL_A \cdot \sin(2\pi f y + \Delta\phi) \\ L_B^*(y) &= L_{Bo}^* + r \cdot AL_B \cdot \sin(2\pi f y) \end{aligned} \tag{8}$$

There are two control variables: One is the phase angle $\Delta\phi$ between the two primary color layers A and B; the other is the ratio r between the banding level in each layer and the AL in the same layer. Note that the AL's used in this part of the experiment are from the same subject as in PART I.

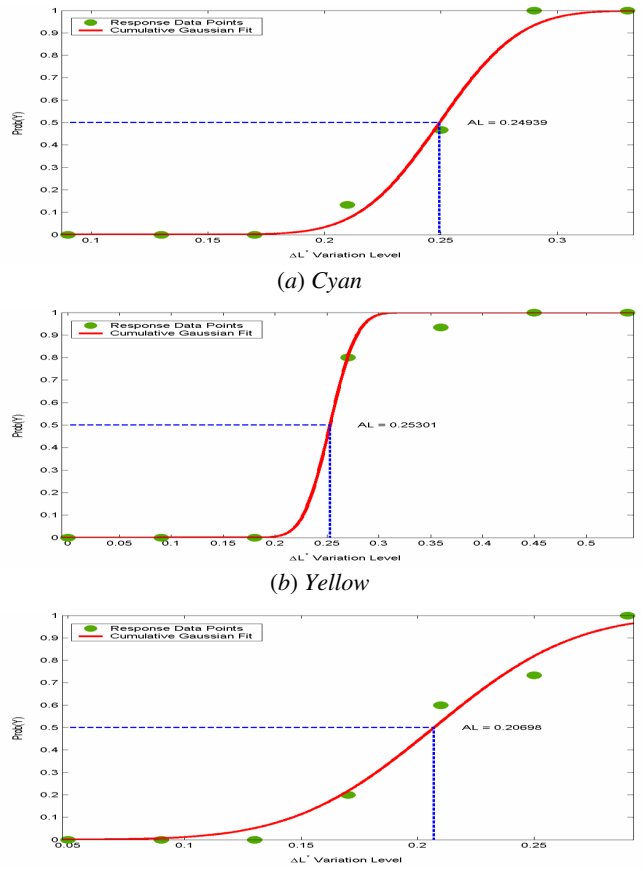

(*a*) *Cyan*

(*b*) *Yellow*

(*c*) *Magenta*

Figure 6. Subject HH's responses to 'seeing banding' in primary color layers

Eight phase angles equally spaced between 0° and 360° were selected. The ratio r has 5 equally spaced levels from 0.2 to 1.0. Again the test patterns are processed by the same 2-D Gaussian filter in PART I in the same manner to form Gabor patches. Including the catch pattern, each test pattern is presented 10 times (totally 410 trials) to the subject in random orders at random positions on the screen. Again, the subject is asked to respond whether s/he sees banding. There is no time limit before the subject makes a choice. The responses are recorded.

Experimental Results

Cyan + Yellow

Figure 7(a) shows the average results among the subjects for the superimposition of the cyan and yellow layers. The vertical axis is the probability of seeing banding. As can be seen the phase angle between banding patterns in the cyan layer and the yellow layer does not have much effect on the perceptibility of chromatic banding. As the banding level in each layer reduces, the probability of perceiving banding decreases, i.e. perceptibility of banding drops. This trend can be expected. From the 2-D illustration we can see that when $r < 0.6$ the perceptibility is below 50%.

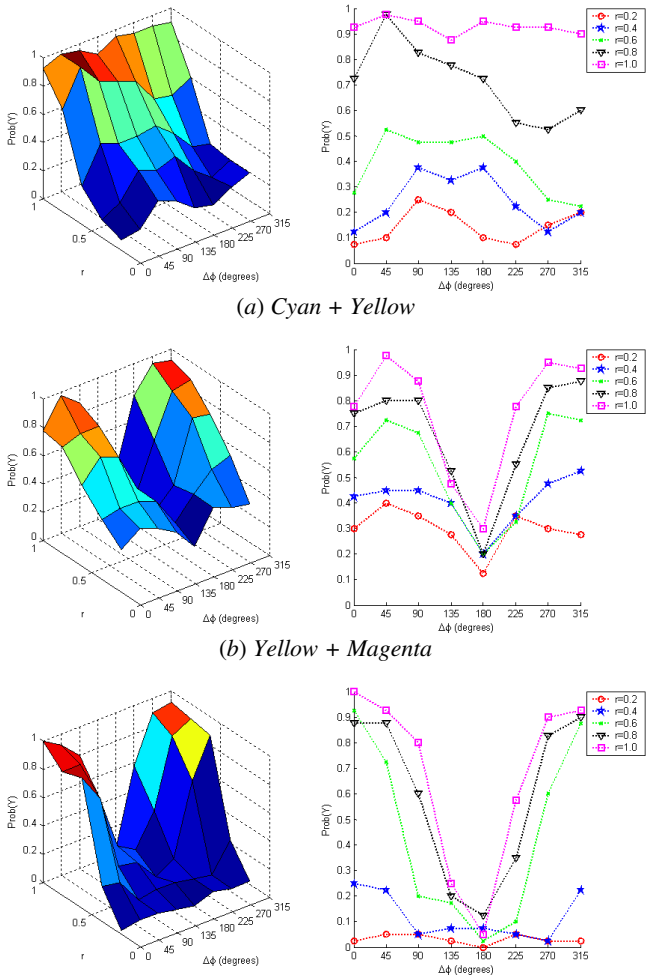

(*a*) *Cyan + Yellow*

(*b*) *Yellow + Magenta*

(*c*) *Magenta + Cyan*

Figure 7. Perceptibility of chromatic banding for the superimpositions of two primary color layers (average results among the subjects)

Yellow + Magenta

Figure 7(b) shows the average results for the superimposition of the yellow and magenta layers. A narrow trough is observed in the 3-D illustration. This is because the perceptibility of chromatic banding decreases when the banding patterns in the yellow layer and magenta layer are 180° out-of-phase. However the maximum perceptibility for a fixed *r* does not necessarily happen when the two banding patterns are in-phase. It happens when the phase difference is around ±50°. Similar to the cyan and yellow, while *r* decreases the perceptibility decreases. To assure the banding perceptibility is below 50%, we need to ensure either $r < 0.4$ or $135° < \phi < 225°$.

Magenta + Cyan

Figure 7(c) shows the average results for the superimposition of the magenta and cyan layers. In the 3-D illustration we see a wider trough for the same reason as explained above for yellow and magenta. When the patterns

in the two layers are in-phase the perceptibility reaches the maximum. For $r < 0.4$ the perceptibility is guaranteed to be less than 50%. For $r > 0.4$, in order to reduce the perceptibility to below 50%, we have to constrain the phase within a certain range around 225°. However this range gets narrower as r gets larger.

In general, the perceptibility of banding in the secondary colors showed that the threshold does not simply added from the primary colors. It can be seen that to ensure the banding perceptibility of less than 50% in the secondary colors, the primary banding level should be no more than 40% of the primary color threshold value. The results illustrated that phase difference between the primary bandings are a factor in the perception of secondary color banding. However, given the nature of the banding signal in EP process, it is unlikely that phase will be an effective parameter, unless some form of synchronization between color planes can be accomplished.

Conclusion

There are two findings from the psychophysical experiments. One is that only controlling the drum speeds individually to suppress the perceptibility of banding in each primary color layer to below 50% will not solve the chromatic banding problem. Banding will show up when they are put back together unless the banding signals are suppressed to below 40% of the threshold for each primary color. The other finding is the combined effect of the amplitude and phase of the banding signal also affects the perceptibility of the banding in the secondary colors. There are many other parameters and scenarios that can be investigated using the similar experiment system. One draw back of the softcopy experiment is that the experiment cannot emulate the effect of laying down primary colors in different order.

Acknowledgement

The authors would like to express their appreciation to the Hewlett-Packard Company for supporting this study.

References

1. G. Y. Lin, J. M. Grice, J. P. Allebach, G. T. C. Chiu, W. Bradburn, and J. Weaver, Banding Artifact Reduction in Electrophotographic Printers by Using Pulse Width Modulation, Journal of Imaging Science and Technology, 46, pp. 326-337, July/August 2002.
2. M. T. S. Ewe, J. M. Grice, G. T. C. Chiu, and J. P. Allebach, C. S. Chan, W. Foote, Banding Artifact Reduction in Electrophotographic Processes Using a Piezoelectric Actuated Laser Beam Deflection Device, Journal of Imaging Science and Technology, 46, pp. 433-442, September/October 2002.
3. C-L. Chen, G. T. C. Chiu, and J. P. Allebach, Banding Reduction in Electrophotographic Process Using Human Contrast Sensitivity Function Shaped Photoreceptor Velocity Control, Journal of Imaging Science and Technology, 47, pp. 209-223, May/June 2003.
4. R. V. Klassen and N. Goodman, Human Chromatic Contrast Sensitivity: Exploration of Dependence on Mean Color, IS&T 8th Color Imaging, pp. 31-38, 2000.
5. N. Goodman, Perception of Spatial Color Variation Caused by Mass Variations about Single Separations, IS&T NIP 14, pp. 556-559, 1998.
6. D. Wulich and N. S. Kopeika, Image resolution limits resulting from mechanical vibrations, Optical Engineering, 26, no. 6, pp. 529-533 (1987).
7. P. D. Burns, M. Rabbani, and L.A. Ray, Analysis of image noise due to position errors in laser writers, Applied Optics, 25, no. 13, pp. 2158-2168 (1986).
8. P. Melnychuck and R. Shaw, Fourier spectra of digital halftone images containing dot position errors, Journal Optical Society of America, 5, no. 8, pp. 1328-1338 (1988).
9. R. P. Loce, W. L. Lama, and M. S. Maltz, Modeling vibration- induced halftone banding in a xerographic laser printer, Journal of Electronic Imaging, 4, no. 1, pp. 48-61 (1995).
10. J. L. Mannos and D. J. Sakrison, The effects of a visual fidelity criterion on the encoding of images, IEEE Trans on Information Theory, IT-20, no. 4, pp. (1974).
11. P. Barten, Evaluation of subjective image quality with the square-root integral method, J. Opt. Soc. Am, 7, no. 10, pp. (1990).

Biography

Mu-Chih Chen received his B.S. degree in Mechanical Engineering from National Taiwan University, Taiwan in 1996 and an M.S. degree in Mechanical Engineering from Purdue University, Indiana in 2001. He is now a Ph.D. candidate in the School of Mechanical Engineering at Purdue University. His fields of interest are digital control and image quality improvement. He has been an IS&T member since 2001.